Response of a Stably Stratified Flow to Cooling

DAVID J. RAYMOND

Physics Department and Geophysical Research Center, New Mexico Institute of Mining and Technology, Socorro, New Mexico

RICHARD ROTUNNO

National Center for Atmospheric Research, Boulder, Colorado*

(Manuscript received 23 July 1988, in final form 25 April 1989)

ABSTRACT

The spreading of the low-level cold pool produced by evaporation of precipitation is generally acknowledged to be an important mechanism for the regeneration of moist convection. We show that cooling a stably stratified nocturnal boundary layer produces very different results from the corresponding daytime case in which the boundary layer is neutral. In particular, dynamic behavior is sometimes closer to that of a gravity wave than to a density current. The gravity wave speed defines a minimum propagation speed for a self-regenerating convective system.

1. Introduction

The possible role of the cool, rain-induced outflow from a thunderstorm in lifting boundary layer air and inducing further convection has long been suspected (Humphreys 1940). Recent observational and numerical work has confirmed this hypothesis, and defined the conditions under which it is most likely to be effective in daytime situations, e.g., Charba (1974), Thorpe et al. (1982), Droegemeier and Wilhelmson (1985a,b), Mueller and Carbone (1987), Rotunno et al. (1988), Weisman et al. (1988). Basically, the cooled air flows away from the parent thunderstorm downdraft. This gravity-driven outflow is called a density current. Air in the path of the density current is lifted, and if a number of conditions are met, a new thunderstorm cell is generated.

Thorpe et al. (1980) studied the response of a predominently unstratified environment to cooling in a fully nonlinear numerical model. They found that a single dimensionless number, the ratio of the ambient wind speed to the spreading speed of the density current in still air, characterized the flow in this case.

Nocturnal thunderstorms play an important role in the weather in a number of regions (Maddox 1980). At night one generally expects to find stable stratification of the atmosphere down to the surface, with the most stable air being at the lowest levels. In this situation it is not clear that the outflow from downdrafts takes on the character of a density current. Rather, the response of the stably stratified fluid to the cooling would, more likely, be in the form of internal gravity waves.

Recently, Smith and Lin (1982), Lin and Smith (1986), Raymond (1986), and Bretherton (1988) studied the response of a stratified atmosphere to imposed heating or cooling. However, these calculations were completely linearized. Crook and Moncrieff (1988) made similar studies in which the atmospheric response was driven by horizontal variations in an applied horizontal force. Both linearized analytic calculations and results of a nonlinear numerical model were presented, and some of the effects we explore here were noted by these authors. However, no attempt was made to systematically map the parameter space.

In this note, we study the nonlinear response of an idealized stratified atmosphere to imposed cooling near the surface. Dimensional and scale analysis lead to *two* pertinent dimensionless numbers rather than the single number found by Thorpe et al. (1980). These numbers are ratios involving three speeds, namely, the approximate spreading speed of the wave of compensating upward motion that results from the imposed cooling, the material outflow velocity were there no stratification, and the ambient wind speed relative to the imposed cooling. With this analysis to guide us, we then perform numerical simulations to explore the nature of the flows in the various regimes.

Since the environment on which the cooling is imposed has no shear and constant static stability, the

* The National Center for Atmospheric Research is supported by the National Science Foundation.

Corresponding author address: Prof. David J. Raymond, Department of Physics, New Mexico Institute of Mining and Technology, Socorro, NM 87801.

results are not directly applicable to thunderstorm environments exhibiting strong low-level shear. As Rotunno et al. (1988) have pointed out, such shear can enhance the development of updrafts induced by density currents. However, the present work has value in defining the theoretical background for studies involving more realistic atmospheric profiles.

2. Theoretical analysis

We imagine a rectangular, continuously cooled region of length l and depth d in a two-dimensional x–z domain, bounded below by a rigid, free-slip surface at $z = 0$. The lower edge of the cooled region is at the surface, and the cooling rate Q is expressed as a buoyancy depletion rate, which gives it the dimensions of acceleration over time. (The buoyancy as we define it is the fractional potential temperature perturbation times the acceleration of gravity.) The cooling is imagined to be due to the evaporation of precipitation. The environment is assumed to be moving uniformly relative to the cooling with a speed U, and has a uniform stratification defined by a constant Brunt frequency, N.

Three dimensionless ratios may be derived from the five parameters l, d, Q, U, and N:

$$F = |U|/(Qdl)^{1/3}, \tag{1}$$

$$G = \pi|U|/Nd, \tag{2}$$

$$A = d/l. \tag{3}$$

We recognize F as the nondimensional number F_N of Thorpe et al. (1980). The combination $(Qdl)^{1/3}$ was found by the above authors to be roughly the speed of advance of the oppositely propagating density currents arising from the above hypothesized cooling in a stationary, unstratified environment. They also found that including an ambient flow U reduced the propagation speed of the upwind density current by of order U, so that the condition $F = F_c \approx 1$ was sufficient to just eliminate upstream propagation. For $F < F_c$, the ambient flow was therefore subcritical relative to density current propagation, while it was supercritical for $F > F_c$. The actual critical value, F_c, was found to be approximately 1.4.

The quantity Nd/π is the horizontal trace speed (in still air) of hydrostatic gravity waves with a vertical wavelength $2d$. A cooled region of depth d will produce gravity waves of all wavelengths, but most of the spectral energy is in vertical wavelengths, and hence speeds, that are larger than these values. However, actual calculations show that a well-defined compensating gravity wave moves horizontally away from suddenly imposed heating or cooling at a speed, relative to the ambient flow, of roughly Nd/π. Thus, $U = Nd/\pi$, or $G = G_c = 1$ also represents a criticality condition: for $G < G_c$, this wave is free to propagate upstream, while for $G > G_c$, it cannot. The two cases are respectively denoted as being subcritical and supercritical relative to gravity wave propagation, even though the meaning is somewhat blurred by the existence of a spectrum of wave speeds in Fourier space.

We now ask how the atmosphere responds when it is stratified. In particular, how does the stratification alter the value U of the environmental wind required to keep a density current from propagating upstream against it? We attempt to answer this question by performing a scale analysis on the steady, linearized, hydrostatic, Boussinesq, two-dimensional, nonrotating equations of motion. Though the details of motion near the head of a density current certainly require a nonhydrostatic treatment, the overall balances that determine density current propagation are essentially hydrostatic. This justifies our use of the hydrostatic approximation. We seek an estimate of the perturbation horizontal velocity, u, in the cooled region, and then ask under what conditions $U + u = 0$ there. This is equivalent to the critical condition at which the upstream propagation of a density current is precisely opposed by the ambient flow. The linearized analysis will not give correct numerical values in this nonlinear limit, but the resulting answer should at least scale correctly.

If the ambient flow is right to left so that $U < 0$, the linearized horizontal momentum equation is

$$U\frac{\partial u}{\partial x} = -\frac{\partial \phi}{\partial x}, \tag{4}$$

where ϕ is the pressure over a constant reference density. Assuming that $u = 0$ at $x = \infty$, then

$$\begin{aligned}\phi^* &\equiv \phi\,(\text{cooled region}) - \phi(\infty)\\ &\approx -Uu\,(\text{cooled region}) \equiv -Uu^*,\end{aligned} \tag{5}$$

by integration of (4) along $z = 0$. Assuming that the pressure anomaly in the cooled region is due primarily to the buoyancy anomaly b^* there, then the hydrostatic equation yields

$$\phi^* \approx -b^*d, \tag{6}$$

where d is the depth of the cooled region. Integrating the buoyancy equation

$$U\frac{\partial b}{\partial x} + wN^2 = -Q \tag{7}$$

in x yields

$$-Ub^* + w^*N^2l \approx -Ql, \tag{8}$$

where we recall that l is the length of the cooled region, w^* is a typical vertical velocity there, and Q is the cooling rate. Finally, from mass continuity we estimate that

$$w^*/d + u^*/l \approx 0. \tag{9}$$

Combining (5), (6), (8), and (9), we find that

$$\frac{u^*}{|U|} \approx \frac{Qld/|U|^3}{[1+(dN/U)^2]} = \frac{F^{-3}}{1+(\pi/G)^2}. \quad (10)$$

A more careful scale analysis would include proportionality constants in (5), (6), (8), and (9). Including these constants and setting $u^*/|U| = 1$ then results in

$$F = F_c = F_0\left[\frac{G^2}{G_0^2+G^2}\right]^{1/3}, \quad (11)$$

where all constants [including the π in (10)] have been incorporated into F_0 and G_0.

In the limit of zero stratification, $G \to \infty$, and $F_c = F_0$. As stratification increases, F_c decreases, which implies that weaker environmental flows succeed in preventing upstream propagation of density currents for a given pattern and strength of cooling period. The physical interpretation is that in the stratified case, some fraction of the cooling is balanced by subsidence, with less being available for producing negative buoyancy. A weaker horizontal density anomaly is therefore created, which diminishes the density current propagation speed. Figure 1 shows how $F = F_c(G)$ and $G = G_c$ divide F–G space into four quadrants with the flow either subcritical or supercritical relative to outflow and waves in each quadrant. For purposes of illustration we have set $F_0 = G_0 = 1$ in this figure. As Thorpe et al. (1980) showed, $F_c = F_0 = 1.4$ in the unstratified case. The other constant, G_0 will be estimated from numerical experiment.

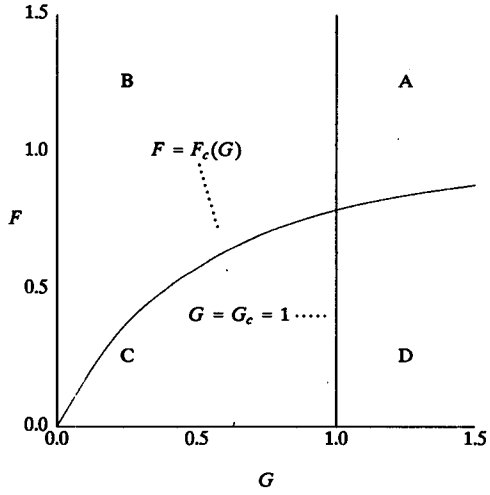

FIG. 1. Regions of F–G space delineated by the theoretical analysis. $F_c(G)$ is plotted from (11) with $F_0 = G_0 = 1$. For $G < G_c$ the flow is subcritical relative to the dominant gravity waves produced by the imposed cooling. For $F < F_c$ the flow is subcritical relative to material outflows. Note that all possible combinations of subcriticality and supercriticality occur. The letters correspond to the section headings in section 4.

It is interesting that the aspect ratio of the cooled region, A, does not show up in the scale analysis. However, it is easy to demonstrate that the hydrostatic governing equations are invariant under the transformation $x \to \epsilon x$, $w \to w/\epsilon$, and $Q \to Q/\epsilon$, where ϵ is a constant scale factor. This transformation changes A, but it doesn't change F or G. Thus, properly scaled solutions to these equations should indeed be independent of A, since the transformed equations would have the same solutions as the original equations.

3. Numerical model

We use the two-dimensional, Boussinesq, hydrostatic, nonrotating numerical model of Raymond (1986), modified to include nonlinear advection. The governing equations are the prognostic equations for vorticity and buoyancy, and the continuity equation:

$$\frac{\partial \zeta}{\partial t} + U\frac{\partial \zeta}{\partial x} + \frac{\partial b}{\partial x} = Y, \quad (12)$$

$$\frac{\partial b}{\partial t} + U\frac{\partial b}{\partial x} + N^2 w = H, \quad (13)$$

$$\frac{\partial u}{\partial x} + \frac{\partial w}{\partial z} = 0. \quad (14)$$

Here U and N are, respectively, the ambient wind and Brunt frequency as before, u and w are the perturbation horizontal and vertical wind components, b is the buoyancy perturbation, and ζ is the vorticity. The ambient buoyancy is given by $N^2 z$, so that the total buoyancy is $N^2 z + b$. Consistent with the hydrostatic approximation, the vorticity is defined

$$\zeta = \frac{\partial u}{\partial z}. \quad (15)$$

The ambient velocity U is assumed constant here, so that the vertical advection of ambient vorticity is absent.

The source terms Y and H include nonlinear advection, mixing terms for unstable lapse rates Y_m and H_m to be discussed below, and in the case of H, the applied buoyancy source H_a:

$$Y = -u\frac{\partial \zeta}{\partial x} - w\frac{\partial \zeta}{\partial z} + Y_m, \quad (16)$$

$$H = -u\frac{\partial b}{\partial x} - w\frac{\partial b}{\partial z} + H_m + H_a. \quad (17)$$

Normally, Y_m and H_m are zero. However, if static instability occurs between any pair of adjacent levels z_i and z_{i+1}, then an additive contribution to Y_m is made of the form

$$Y_m(z_{i+1}) = [\zeta(z_i) - \zeta(z_{i+1})]/\tau \quad (18)$$

$$Y_m(z_i) = [\zeta(z_{i+1}) - \zeta(z_i)]/\tau, \quad (19)$$

with a similar contribution being made to H_m. This has the effect of mixing material between these levels, with a consequent tendency to drive gradients to zero. The characteristic mixing time τ is not critical as long as it is larger than the integration time step, but smaller than the characteristic time of the rest of the calculation. A value $\tau = 2$ was found to be satisfactory. The mixing terms are rarely activated in the present computations.

The equations are scaled in length by an arbitrary scaling length L, and in time by the inverse of the Brunt frequency, N^{-1}. If $L = 6$ km and $N^{-1} = 100$ s, then the scaling velocity is 60 m s^{-1}. The scaling buoyancy is 0.6 m s^{-2}, or about 18°C in terms of potential temperature. The scaling buoyancy sink is 6×10^{-3} m s^{-3}, or 0.18°C s^{-1}.

Solution of (12)–(15) is by the same method as in Raymond (1986). The x and z grid intervals are respectively 1 and 0.05, and the computational domain is [0, 40] in x and [0, 1] in z. Radiation upper boundary conditions are imposed, and lateral boundary conditions are periodic, with a repetition length that is large enough to prevent significant wraparound. The integration time step is set to 0.4.

The source terms are computed only in a restricted subdomain in x of [0, 20], and are assumed to be zero outside this region. This saves substantial computer time, and test simulations show that it causes negligible error as long as the strongest motions are confined to the subdomain. For the sake of simplicity, advection is computed using upstream and forward differencing. In cases where the nonlinearity is weak, the results are better than normally expected from upstream differencing because only the *nonlinear* part of the advection is computed this way—the linear part is included on the left sides of (12) and (13). Halving the x and z grid spacing as well as the time step had no effect on the results other than to slightly sharpen gradients, which suggests that the mixture of first and second order methods cause no significant errors.

The nonlinear advection was tested by simulating a density current in an unstratified environment. This is a much more stringent test of the numerical method than is presented by outflows in the stratified case, where a large fraction of the advection is linear. Density current speeds comparable to those predicted by Benjamin (1968) are obtained.

4. Results of simulations

A large number of simulations were made to determine the character of the function $F_c(G)$. The simulations were performed as initial value problems, with cooling turned on at time $t = 0$. The form of the cooled region (shown in Fig. 2) was the same for all simulations. It consisted of uniform cooling of strength $H_a = -Q$ with width $l = 3$ and depth $d = 0.5$, extending from the surface upward. Thus, the aspect ratio A of

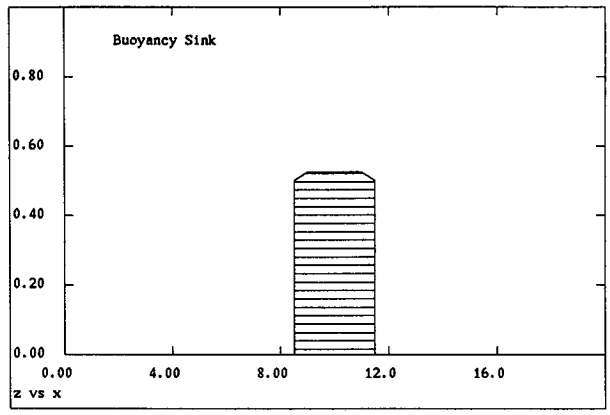

FIG. 2. Position and geometry of the applied buoyancy sink for the numerical simulations. The width $l \approx 3$, while the depth $d \approx 0.5$.

the cooling was held constant. The parameters varied were Q and the strength of the (uniform) ambient wind, U. The parameters F and G were calculated from (1) and (2). Simulations were integrated out to $t = 100$ and the evolution of the flow was examined. By this time nearly steady behavior had generally developed in the vicinity of the cooled region, though continued evolution of gravity waves and the material outflow often was occurring well away from this region. (Lin and Smith 1986, showed that a true steady state is never reached in this situation, and Bretherton 1988, explained why this is so; thus the caveat "nearly.") The flow was judged to be subcritical relative to material outflow if reversed flow had developed somewhere at $z = 0$ by the end of the simulation.

Table 1 shows the results of these simulations. Figure 3 plots the results in the F–G plane, along with the $F_c(G)$ curve from (11), with $F_0 = 1.4$ and $G_0 = 1.65$. Simulations with reversed flow (i.e., subcritical) are indicated by × while supercritical flows are indicated by a circle. Recall that (11) defines the boundary between subcriticality and supercriticality in the material outflow. Figure 3 thus shows good agreement between the simulation results and the theory for the above choice of parameters. Since the value of F_0 was taken from the earlier results of Thorpe et al. (1980), only G_0 was adjusted to obtain the fit shown.

We now examine sample simulations from each of the four regions defined in Fig. 1.

a. Supercritical relative to waves and outflow

Figure 4 shows the flow in the x–z plane at $t = 100$ for test 7, which is supercritical relative to both compensating wave motion and to material outflow. Only the flow at this time is shown, as the flow quickly comes to a steady state. Note that the response to the cooling is an isolated wave of elevation at low levels, becoming a wave of depression aloft, due to the upstream tilt of

TABLE 1. Results of simulations. F and G are calculated assuming $l = 3$, $d = 0.5$, and $N = 1$. The column "reversed flow" is "yes" if flow opposed to the mean flow is generated at the surface during the period of the simulation.

Test	U	Q	F	G	Reversed flow
1	−0.08	0.005	0.515	0.50	yes
2	−0.08	0.01	0.409	0.50	yes
3	−0.08	0.02	0.324	0.50	yes
4	−0.08	0.04	0.257	0.50	yes
5	−0.08	0.002	0.699	0.50	no
6	−0.08	0.001	0.880	0.50	no
7	−0.24	0.005	1.545	1.51	no
8	−0.24	0.01	1.226	1.51	no
9	−0.24	0.02	0.973	1.51	yes
10	−0.24	0.05	0.717	1.51	yes
11	−0.16	0.002	1.398	1.01	no
12	−0.16	0.005	1.030	1.01	no
13	−0.16	0.01	0.817	1.01	yes
14	−0.04	0.0002	0.753	0.25	no
15	−0.04	0.0005	0.555	0.25	no
16	−0.04	0.001	0.440	0.25	no
17	−0.04	0.002	0.349	0.25	yes

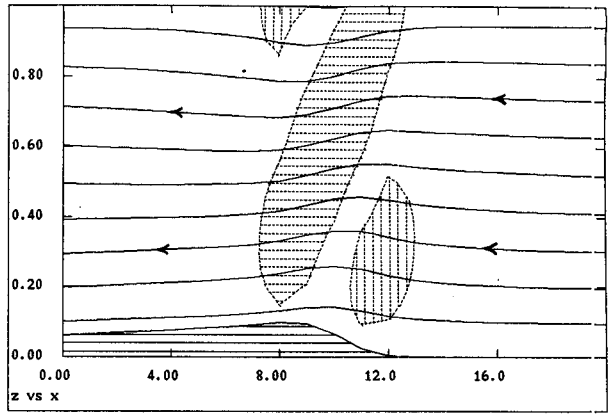

FIG. 4. Results of test 7 (supercritical relative to both waves and material outflow) at $t = 100$. Streamlines are shown by solid lines in the x–z plane, while dashed hatching shows regions of significant vertical motion. Vertical hatching indicates $w > 0.0025$, while horizontal hatching indicates $w < -0.0025$. Solid horizontal hatching shows the cold pool, i.e., that region with negative total buoyancy.

the phase surfaces. The cold pool (defined as that region with negative total buoyancy, $N^2z + b$) is shown by the horizontally hatched region at low levels. Note that it does not push upstream of the region of cooling, which is defined in Fig. 2. This is consistent with the absence of reversed flow. The updraft and downdraft are roughly the same strength at low levels, with the updraft sitting just upstream of the downdraft, or on the upstream edge of the cooling.

b. *Subcritical relative to waves, supercritical relative to outflow*

When the flow is subcritical relative to waves, but still supercritical relative to outflow, a very different flow pattern results. Test 6 fits this pattern, and the flow at $t = 100$ is shown in Fig. 5 for this case. The only strong vertical motion is a downdraft in the cooled region. The compensating updraft moves upstream and becomes broader and weaker with time. In the long time limit (with a nonperiodic domain) one would likely see it become very broad and weak, with nearly horizontal streamlines everywhere except in the cooled region. The strength of the downdraft is roughly that required to restore buoyancy equilibrium with the environment in the face of the imposed cooling. As expected, the cold pool does not push upstream of the buoyancy sink.

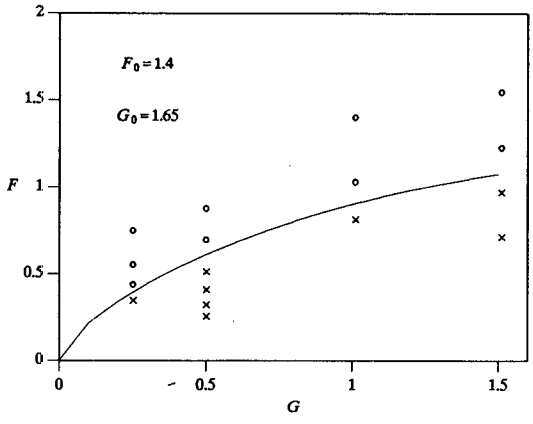

FIG. 3. Results of numerical simulations plotted in F–G plane. The function $F_c(G)$, obtained from (11) with $F_0 = 1.4$ and $G_0 = 1.65$, is shown by the solid line. Simulations with supercritical flow relative to material outflow (i.e., no flow reversal at low levels) are plotted with a circle, while those with subcritical flow are shown by ×.

c. *Subcritical relative to waves and outflow*

We modify the above simulation by increasing Q by a factor of 5 while keeping U the same. The result is

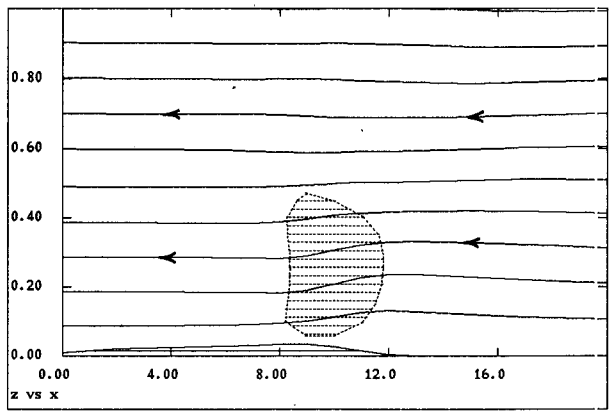

FIG. 5. Results of test 6 (subcritical relative to waves, supercritical relative to material outflow) at $t = 100$. Contouring as in figure 4 except dashed hatching indicates $|w| > 0.0005$.

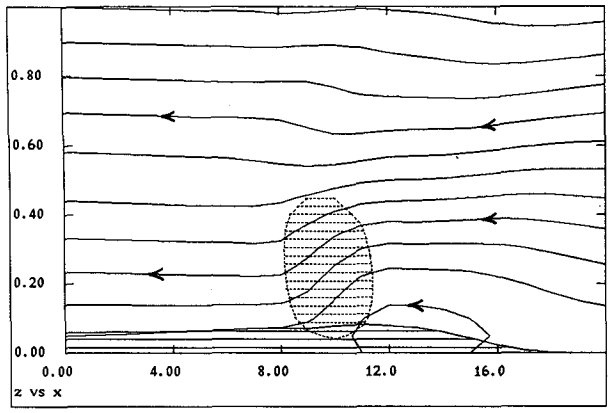

FIG. 6. Results of test 1 (subcritical relative to both waves and material outflow) at $t = 100$. Contouring as in Fig. 4 except dashed hatching indicates $|w| > 0.0025$.

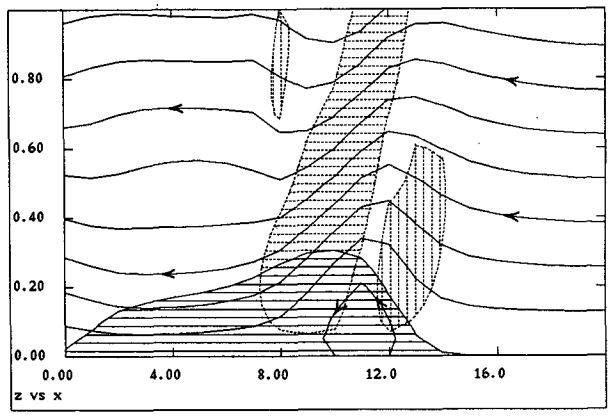

FIG. 8. Results of test 10 (supercritical relative to waves, subcritical relative to material outflow) at $t = 20$. Contouring as in Fig. 4 except dashed hatching indicates $|w| > 0.01$.

test 1, with flow subcritical relative to both waves and material outflow. Figure 6 shows the flow at $t = 100$. We note that the pattern is similar to the previous case (test 6) except that the vertical displacements increase and a region of reversed flow develops upstream of the cooled region. The cold pool extends to near the upstream edge of the reversed flow region, as would be expected by advection.

Figure 7 shows the upstream propagation of the cold pool at $z = 0$ in the t–x plane. The hatched region indicates total buoyancy less than -0.05, and the arrows indicate the total horizontal wind, $U + u$. Comparable upstream propagation does not exist in the previous test (test 6).

Perhaps the most surprising result of this test is how little the cold pool affects the vertical velocity field. In comparison with Fig. 5, Fig. 6 shows only slight concentration of upward motion over the leading edge of the cold pool. Qualitatively, the patterns of the two figures are very similar, with the downdraft in the cooled region dominating the vertical velocity field.

d. Supercritical relative to waves, subcritical relative to outflow

This final case is represented by test 10. Figures 8 and 9 show the flow pattern at $t = 20$ and $t = 60$, respectively. As expected, the material outflow propagates upstream relative to the ambient wind. In this case significant upward motion is located at the upstream edge of the material outflow. The downdraft

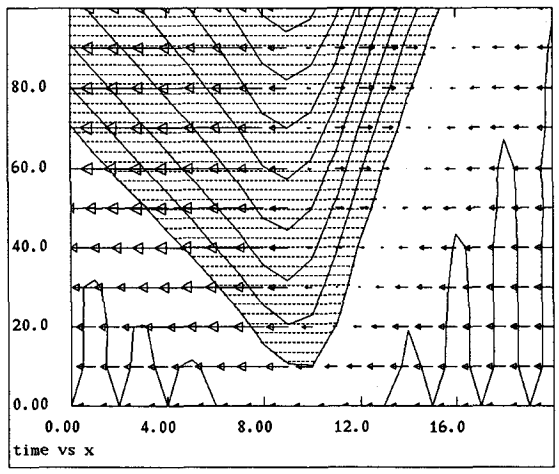

FIG. 7. Surface wind and buoyancy for test 1. Total buoyancy is shown in the x–t plane at $z = 0$ by contours with interval 0.05. Hatching highlights regions with total buoyancy less than -0.05, and roughly defines the bounds of the cold pool. The arrows indicate the horizontal wind at $z = 0$, with an arrow equal in length to one x grid interval indicating a dimensionless velocity of 0.1. Recall that the ambient wind is 0.08 in this case. Note the reversed flow at the leading edge of the cold pool.

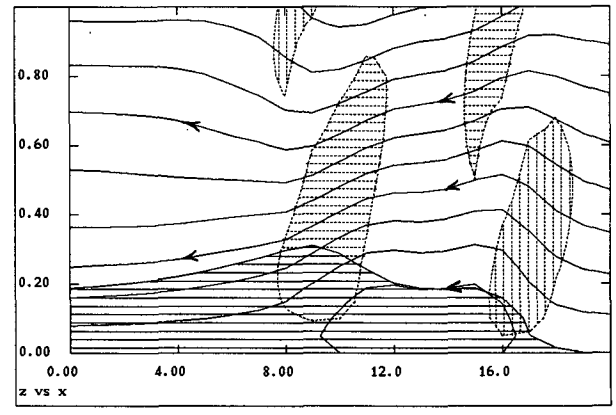

FIG. 9. As in Fig. 8, except $t = 60$. Note how the material outflow has moved upstream in this case. The strongest upward motion is located on the upstream edge of the material outflow.

remains in the vicinity of the imposed cooling. The cold pool is much deeper in this case because very strong cooling is required to produce a material outflow that spreads faster than the compensating wave in a stably stratified environment.

Of all the cases, this one most resembles a density current in an unstratified medium. This may be seen by comparison with Fig. 10, which shows the flow due to imposed cooling with $N = 0$ for $z < 0.9$ and $N = 1$ above. The size and shape of the cooled region is the same as in the above simulations, while $Q = 0.002$ and $U = 0.05$. This results in infinite G and $F = 0.437$ according to (3) and (4), with k, l, and d set to the above-defined values.

5. Discussion

It is clear from the above simulations that wave effects can modify the response to imposed cooling when the environment is stratified. The result resembles a density current only when the cooling is strong enough to produce an outflow that spreads faster than the compensating gravity waves.

Let us put some numbers into the model that are characteristic of thunderstorm downdrafts. If the depth of the cooled region is 3 km and the Brunt frequency is 10^{-2} s^{-1}, then the dominant wave speed is $Nd/\pi = 9.5$ m s^{-1}. The scaling velocity of the simulation is twice the depth of the cooled region times the Brunt frequency, or 60 m s^{-1}, and a dimensionless width $l = 3$ translates to 18 km in dimensional terms. Equation (7) may be used to estimate equilibrium downdraft strengths, with the result that $Q = 0.002$ corresponds to $w = -1.2$ m s^{-1}. These values are typical of what might be found in a small mesoscale downdraft.

We estimate that the density current speed in an unstratified environment is $(Qld)^{1/3} = 8.7$ m s^{-1}, given the above parameter values. Stratification can only decrease the speed of a density current. Thus, the material outflow speed is less than or equal to 90% of the dominant wave speed for this case, and the flow can never be simultaneously supercritical relative to waves and subcritical relative to material outflow. The system is thus limited to a choice of one of the other three possibilities, depending on U.

In order to increase the material outflow speed relative to the wave speed, one needs to increase the product Ql or decrease N or d. This is easily seen by computing the ratio of the two speeds

$$\frac{(Nd/\pi)}{(Qld)^{1/3}} = \frac{Nd^{2/3}}{\pi(Ql)^{1/3}}. \tag{20}$$

The dependence of the above equation on Ql to the one third power makes changes in this quantity relatively ineffective in altering the ratio. However, a shallow downdraft (say, $d < 1$ km) may allow this ratio to fall below unity, as would a very large scale downdraft that greatly increased l.

For a convective system to be self-maintaining via the downdraft mechanism, new convection, and hence substantial lifting, must be induced just upstream of the downdraft. In this way precipitation will be transported into the downdraft region, thus providing a mechanism for its continued existence. Oscillating systems such as those simulated by Rotunno et al. (1988) may have instantaneous configurations that differ from this pattern, but must have this structure on the average.

The results of the previous section show that lifting occurs just upstream of the cooled region only when the flow is supercritical relative to compensating waves. In other words, the propagation speed of the system relative to the low-level air must exceed the dominant wave speed, or 9.5 m s^{-1} in the above example. If material outflow speeds are greater than this value, lifting will occur over the upstream edge of the outflow. If not, the wave will be primarily responsible for the lifting under the stated conditions.

The existence of a minimum propagation speed distinguishes nocturnal systems from those that occur over a neutral boundary layer during the day. In the latter case, density current speeds vary monotonically with the intensity of the forcing, and no clear-cut lower bound exists.

As noted in the Introduction, application of these results to the real world must be tempered by the knowledge that they strictly apply only to situations with constant stability and wind. Exploration of the effects of evaporative cooling on real nocturnal atmospheric profiles remains to be done.

Acknowledgments. We wish to thank the reviewers, whose clarifications and corrections greatly enhanced the quality of this paper. This work was supported by

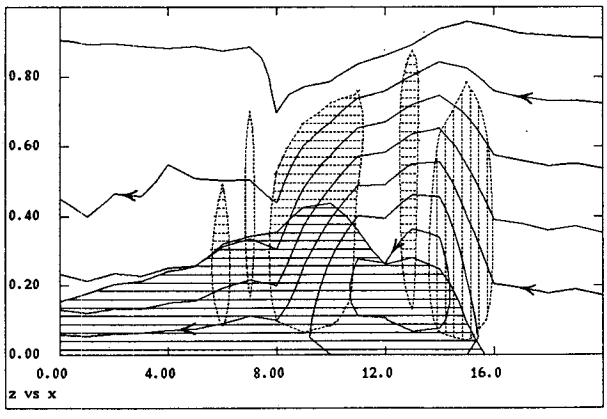

FIG. 10. Flow pattern at $t = 100$ for the case of an unstratified environment below $z = 0.9$. Parameter values are $U = 0.05$ and $Q = 0.002$, resulting in $F = 0.437$. Streamlines are given by solid lines while dashed hatching shows vertical velocities with $|w| > 0.005$. The cold pool is approximately bounded by the total buoyancy contour of 0.88, and is indicated by the horizontal long-dashed region. Note the resemblance of this pattern to Fig. 9.

National Science Foundation grants ATM-8611364 and ATM-8605136.

REFERENCES

Benjamin, T. B., 1968: Gravity currents and related phenomena. *J. Fluid Mech.*, **31,** 209–248.

Bretherton, C., 1988: Group velocity and the linear response of stratified fluids to internal heat or mass sources. *J. Atmos. Sci.*, **45,** 81–93.

Charba, J., 1974: Application of gravity current model to analysis of squall-line gust front. *Mon. Wea. Rev.*, **102,** 140–156.

Crook, N. A., and M. W. Moncrieff, 1988: The effect of large-scale convergence on the generation and maintenance of deep moist convection. *J. Atmos. Sci.*, **45,** 3606–3624.

Droegemeier, K. K., and R. B. Wilhelmson, 1985a: Three-dimensional numerical modeling of convection produced by interacting thunderstorm outflows, Part I: Control simulation and low-level moisture variations. *J. Atmos. Sci.*, **42,** 2381–2403.

——, and ——, 1985b: Three-dimensional numerical modeling of convection produced by interacting thunderstorm outflows, Part II: Variations in vertical wind shear. *J. Atmos. Sci.*, **42,** 2404–2414.

Humphreys, W. J., 1940: *Physics of the Air.* Dover, 676 pp.

Lin, Y. L., and R. B. Smith, 1986: Transient dynamics of airflow near a local heat source. *J. Atmos. Sci.*, **43,** 40–49.

Maddox, R. A., 1980: Mesoscale convective complexes. *Bull. Amer. Meteor. Soc.*, **61,** 1374–1387.

Mueller, C. K., and R. E. Carbone, 1987: Dynamics of a thunderstorm outflow. *J. Atmos. Sci.*, **44,** 1879–1898.

Raymond, D. J., 1986: Prescribed heating of a stratified atmosphere as a model for moist convection. *J. Atmos. Sci.*, **43,** 1101–1111.

Rotunno, R., J. B. Klemp and M. L. Weisman, 1988: A theory for strong, long-lived squall lines. *J. Atmos. Sci.*, **45,** 463–485.

Smith, R. B., and Y. L. Lin, 1982: The addition of heat to a stratified airstream with application to the dynamics of orographic rain. *Quart. J. Roy. Meteor. Soc.*, **108,** 353–378.

Thorpe, A. J., M. J. Miller and M. W. Moncrieff, 1980: Dynamical models of two-dimensional downdraughts. *Quart. J. Roy. Meteor. Soc.*, **106,** 463–484.

——, —— and ——, 1982: Two-dimensional convection in non-constant shear: A model of mid-latitude squall lines. *Quart. J. Roy. Meteor. Soc.*, **108,** 739–762.

Weisman, M. L., J. B. Klemp and R. Rotunno, 1988: The structure and evolution of numerically simulated squall lines. *J. Atmos. Sci.*, **45,** 1990–2013.